



## A Solar Timber Drying System: Experimental Performance and System Modeling

[www.ericjournal.ait.ac.th](http://www.ericjournal.ait.ac.th)

S. Janjai\*<sup>1</sup>, P. Intawee\*, J. Kaewkiew\*

**Abstract** – This paper presents experimental and simulated performance of a solar timber drying system. The system consists of a solar collector on the top and a drying unit at the bottom. These are connected in series through U-turn at both ends. Hot air from the collector is forced by three fans to dry timber arranged in stacks in the drying unit. The air leaving the drying unit is exhausted with a provision to recirculate partially as needed. One full scale experiment was conducted to assess the drying potentials of the solar drying system. The average temperature rise at inlet of drying unit was 8 °C and the timber was dried from 25 % to 12.2% (db) moisture content within 12 days. In order to obtain the moisture diffusivity of the timber for the simulation of drying system, timber in the form of a slab was dried under controlled conditions of temperature and relative humidity in a laboratory dryer. The diffusivity was determined by minimizing the sum of the square of the deviation between the predicted and experimental values of the moisture content of the timber. It was found that the diffusivity increased with temperature and it can be expressed as a function of the temperature using the Arrhenius type equation. For the system modeling, two sets of equations were used to describe the heat and mass transfer inside the collector and the drying unit and these were numerically solved using the finite difference method. The values of the predicted moisture content and those obtained from the experiment were in reasonable agreement. The payback period of this drying system is 3.6 years.

**Keywords** – Diffusivity, modeling, simulation, solar dryer, timber.

### 1. INTRODUCTION

Timber is still the most popular choice as construction materials for doors and windows and furniture in buildings although metals and synthetics are available. For production of quality timber, it must be properly dried to a desired moisture content without any crack and deformable stress. In terms of energy consumption, drying of timber is an energy intensive operation. In general, the energy required for drying timber in conventional dryer ranges from 600 to 1,000 kWh/m<sup>3</sup> depending on types of timber and its thickness [1]. Thailand being located in the tropics, it has abundant of solar radiation [2]. Therefore, the obvious option for drying of timber is solar drying.

Solar drying is an elaboration of sun drying and an efficient method of utilization of solar energy [3]. Many studies have been reported on drying of timber [1], [4]-[10]. Also several studies have been reported on modeling of drying of timber [1], [5], [7]-[8], [10]-[15]. Helwa *et al.* [6] reported experimental evaluation of a semi-greenhouse solar dryer and the experimental results show that timber boards were dried inside solar kiln to a moisture content of 12%(db) within 17 days, whereas for air drying of timber, moisture content was limited to 20% for the same period. Haque and Langrish [9] also reported the performance of an industrial solar kiln for drying of timber and it was considered as an acceptable alternative to the air-drying method for the pre-drying of hard woods. Minea [16] reported the development of industrial and laboratory scale soft wood

dryers with high temperature heat pump and tested in a field level. The energetic performance of this soft wood dryer with high temperature heat pump was relatively high. Awadalla *et al.* [8] reported a finite element simulation of drying timber. Their computed results were in considerable agreement with previous experimental and theoretical results. Pang [10] developed mathematical models of kiln drying of soft wood timber and the models can be divided into three categories: models for drying a single board, models for drying a kiln-wide stack and models for drying stress and deformation and also reported that an integrated model can be used to optimize drying schedules and develop strategies for high quality dried timber. Younsi *et al.* [15] reported heat and mass transfer during high temperature heat treatment of wood using finite element method and the agreement between the numerical and experimental results was good. Haque and Langrish [5] reported a complete solar kiln model and compared the predicted internal air temperatures, relative humidities, and timber moisture contents with experimental data. The agreement between the predicted and observed results were reasonable. Khater *et al.* [7] reported theoretical investigation of the physical process of solar drying of timber based on conventional heat and mass transfer equations and the model was simulated using the finite difference technique that is based on an object oriented approach. Ceylan *et al.* [17] reported energy and exergy analysis of timber dryer assisted heat pump and determined the energy utilization and exergy losses during the drying process. More recently Luna *et al.* [18] presented an analysis of the evolution in solar heated drying kilns in the recent decades which show that there have been a series of modifications to optimize the

\*Solar Energy Research Laboratory, Department of Physics, Faculty of Science, Silpakorn University, Nakhon Pathom 73000, Thailand.

<sup>1</sup>Corresponding author; Tel.: +66-34-270 761; Fax: +66-34-271 189.  
E-mail: [serm@su.ac.th](mailto:serm@su.ac.th)

thermal and drying efficiency and also suggested some future adaptations.

Performance of solar drying of timber can be studied by full scale experiments on solar drying for different configurations of the kilns and for different types of timber. Conducting full scale experiments for different configurations and types of timber are expensive and time consuming. Most inexpensive and less time consuming method is to use mathematical models.

Mathematical modeling of timber drying is a powerful tool to better understand the transfer processes and also to quantify the effects of drying on the properties of the wood and hence the quality of timber as construction materials. This study focuses on determination of diffusivity of timber and investigation of experimental and simulated performance of a solar timber drying system.

## 2. DETERMINATION OF DIFFUSIVITY OF TIMBER

Single layer drying of timber boards was conducted using a laboratory dryer under controlled conditions of temperature and relative humidity at the Department of Physics, Silpakorn University. The laboratory dryer used here is similar to that described by Guarte *et al.* [19]. The laboratory dryer consists of a ceramic packed-bed for producing saturated air at a given temperature, an

electrical heater, a blower, a drying section, measurement sensors and a data recording and controlling system with a personal computer (Figure 1). In this laboratory dryer, the blower forces ambient air through a humid ceramic packed-bed. The air absorbs moisture while it passes through the packed-bed. At the top of the packed-bed, this air leaves humidified. Then this saturated air is heated by the air heater and passed through the timber stacks, the relative humidity and temperature of the drying air are controlled by adjusting the power supply to the air heater and the water heater using a psychrometric chart as a guideline.

Prior to an experiment the laboratory dryer was allowed to run for half hour to obtain steady temperature. For each experiment, a timber board of 0.12 m × 0.09 m × 0.02 m was used for single layer drying. All the drying experiments were carried out at an air velocity of 0.5 m/s. The drying air temperatures were monitored using a thermocouple (K type) connected to a personal computer using an interface at an interval of 5 minutes and the weight of timber board was recorded by an electronic balance (accuracy ± 0.01 g) at an interval of one hour. The single layer drying tests were conducted in the temperature range of 40°C to 60°C and the relative humidity of the drying air from 10 to 25%. Three sets of experiments were conducted for the timber board.

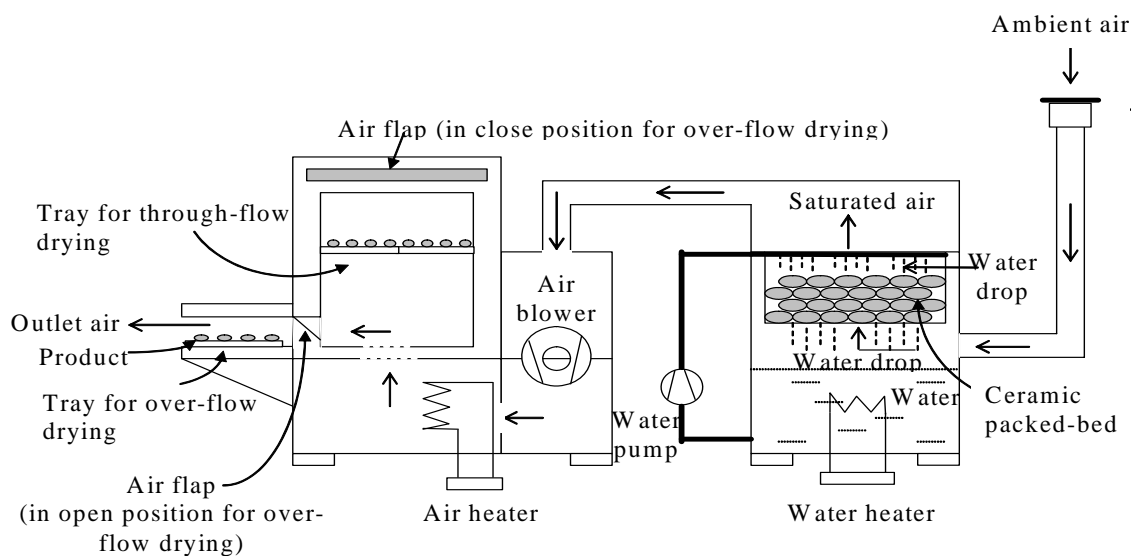


Fig. 1. Schematic diagram of the laboratory dryer.

Fick's second law of the unsteady state diffusion, neglecting the effects of temperature and total pressure gradient, can be used to describe the drying behavior of timber [3].

$$\frac{\partial M}{\partial t} = \text{Div}(D_w \text{grad } M) \quad (1)$$

where  $M$  is the moisture content,  $D_w$  is the moisture diffusivity of timber and  $t$  is time.

This equation can be solved for different standard shapes of the drying material. The solution for a slab of timber is:

$$\frac{M - M_e}{M_o - M_e} = \frac{8}{\pi^2} \sum_{n=1}^{\infty} \frac{4}{(2n-1)^2} \exp\left(- (2n-1)^2 \frac{D_w t}{z^2}\right) \quad (2)$$

where  $M_e$  is equilibrium moisture content of timber,  $M_o$  is initial moisture content of timber,  $n$  is the order of the infinite series and  $z$  is the distance from the center of the slab.

Equation 2 was fitted to the experimental data of the timber for the shape of a slab and the diffusivity was determined by minimizing sum of squares of the deviation between the predicted and experimental data. The results are presented in Section 5.

### 3. EXPERIMENTAL SET-UP AND PROCEDURE FOR TIMBER DRYING

#### Experimental set-up

The solar drying system used in this study was constructed at Silpakorn University, Nakhon Pathom (13.82 °N, 100.04 °E), Thailand. The pictorial view of the dryer is shown in Figure 2. The dryer consists of a

solar collector on the top and drying unit at the bottom. The back-insulator of the collector served as the top of the drying unit. The required air flow was provided by three axial flow fans. The ambient air was forced through the collector at the top of the dryer and at the end of the collector the air was forced through the timber arranged in stacks through a U-turn. The air leaving the dryer was exhausted with provision of partially recirculate. In this study, 90% of the air leaving the drying unit was recirculated throughout the drying experiment. The movement of the air inside the collector and the drying unit, and the dimension of the drying system are shown in Figure 3.



Fig. 2. Pictorial view of the solar timber drying system.

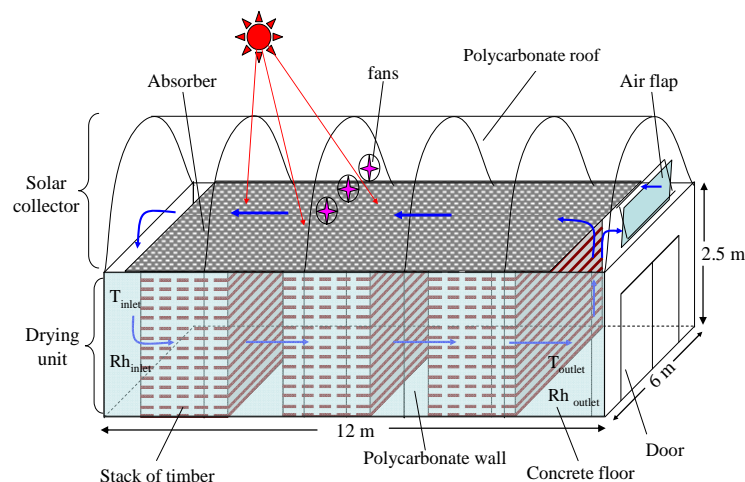


Fig. 3. Solar timber drying system.

#### Experimental Procedure

Full scale drying of timber in the solar dryer was conducted in 2006. The soft wood timber was used for the experiment. Boards of the timber were placed into three stacks with a gap between the boards of 0.025 m. Each timber board has a dimension of 0.025 m  $\times$  0.15 m  $\times$  3.50 m. One thousand timber boards with an initial moisture content of 25% (db) were dried in the solar timber drying system.

The solar radiation, temperatures and relative humidity inside dryer as well as outside of the dryer were measured at an interval of 10 minutes. A pyranometer of Kipp and Zonen (model CM11) was used to measure solar radiation. The temperatures inside the dryer were measured using K-type thermocouples (accuracy  $\pm 2\%$ ) and the relative humidity of the air was measured using hygrometers (Elektronik, model EE23, accuracy,  $\pm 2\%$ ). The positions of the measurements of

temperature and relative humidity inside the dryer are shown in Figure 3. Signals from the pyranometer, hygrometers and thermocouples were recorded by a data logger of Yagokawa (model DC100) every 10 minutes. The air flow rate was also manually monitored at an interval of 1 hour using an anemometer (Airflow, model TA5, accuracy,  $\pm 2\%$ ). The weight changes of timber samples were measured at an interval of 1 hour using an electronic balance (KERN model 474, accuracy,  $\pm 0.01$  g). The dry solid mass of the samples was determined by using the oven method. This mass was used to estimate the moisture content of the timber.

#### 4. MATHEMATICAL MODELING OF THE DRYING SYSTEM

##### Formulation of the Model

The following assumptions were used for the formulation of the model. These are: i) air flow is one dimension, ii) specific heats of the dry air and dry products are constants, iii) moisture movement inside the timber is by diffusion and it is one dimensional, iv) shrinkage of timber during drying is negligible and v) heat loss from the absorber of the collector to the drying unit is negligible.

Heat and mass balance equations are given below.

##### Energy Balance for the Polycarbonate Roof

The energy balance for the polycarbonate roof can be written as:

Rate of thermal energy accumulated in the roof = Rate of convective heat transfer between the roof and air inside the collector + Rate of convective heat transfer between the roof and ambient air + Rate of radiative heat transfer between the roof and the sky + Rate of radiative heat transfer between the absorber and the roof + Rate of solar radiation absorption in the roof

$$\begin{aligned} m_r C_{pr} \frac{dT_r}{dt} &= A_r h_{c,r-a} (T_{a1} - T_r) \\ &+ A_r h_{c,r-am} (T_{am} - T_r) + A_r h_{r,s} (T_s - T_r) \\ &+ A_r h_{r,ab-r} (T_{ab} - T_r) + A_r I \alpha_r \end{aligned} \quad (3)$$

##### Energy Balance for the Air Inside Collector

The energy balance for the air inside the collector is expressed as: Rate of enthalpy change in the air stream = Rate of convection heat transfer between the air and the roof + Rate of convective heat transfer between the air and the absorber

$$D_c G C_{pa} \frac{dT_{a1}}{dx} = h_{c,r-a} (T_r - T_{a1}) + h_{c,ab-a} (T_{ab} - T_{a1}) \quad (4)$$

##### Energy Balance for the Absorber

The energy balance for the absorber can be written as: Rate of thermal energy accumulation in the absorber = Rate of convective heat transfer between the absorber and air in the collector + Rate of radiative heat transfer between the absorber and the roof + Rate of radiant energy absorbed by the absorber

$$\begin{aligned} m_{ab} C_{pab} \frac{dT_{ab}}{dt} &= A_{ab} h_{c,ab-a} (T_{a1} - T_{ab}) \\ &+ A_{ab} h_{r,ab-r} (T_r - T_{ab}) + A_{ab} \alpha_{ab} \tau_r I_t \end{aligned} \quad (5)$$

##### Energy Balance for the Air Inside Dryer

The energy balance for the air inside the dryer can be expressed as: Rate of accumulation of thermal energy in the air inside the drying unit = Rate of thermal energy transfer between the timber and air in the drying unit due to convection + Rate of thermal energy transfer between the floor and the air in the drying unit due to convection + Rate of thermal energy gain of the air from timber due to sensible heat transfer from the product to the air + Rate of thermal energy gained in the drying unit due to inflow and outflow of the air in the drying unit + Rate of overall heat loss from the air in the drying unit to ambient air + Rate of solar energy accumulation inside the drying unit from solar radiation:

$$\begin{aligned} m_a C_{pa} \frac{dT_{a2}}{dt} &= A_w h_{c,w-a} (T_w - T_{a2}) \\ &+ A_f h_{c,f-a} (T_f - T_{a2}) \\ &+ A_w DC_{pv} \rho_w (T_p - T_{a2}) \frac{dM_w}{dt} \\ &+ (\rho_a V_{out} C_{pa} T_{out} - \rho_a V_{in} C_{pa} T_{in}) \\ &+ U_c A_c (T_{am} - T_{a2}) + [1 - \alpha_f F_f - \alpha_w F_w] I_t A_c \tau_c \end{aligned} \quad (6)$$

##### Energy Balance for the Floor

The energy balance for the floor is: Rate of accumulation of thermal energy in the floor = Rate of convective heat transfer between the floor and air in the drying unit + Rate of conductive heat transfer from the floor to the ground + Absorbed solar radiation

$$\begin{aligned} m_f C_{pf} \frac{dT_f}{dt} &= A_f h_{c,f-a} (T_{a2} - T_f) \\ &+ A_f h_{D,f-g} (T_g - T_f) + \alpha_f F_f I_t A_f \tau_c \end{aligned} \quad (7)$$

##### Energy Balance of the Timber

Rate of accumulation of thermal energy in the timber = Rate of thermal energy received from air by the timber due to convection + Rate of thermal energy lost from the timber due to sensible and latent heat loss from the timber + Rate of thermal energy absorbed by the timber

$$\begin{aligned} m_w (C_{pw} + C_{pl} M_w) \frac{dT_w}{dt} &= A_w h_{c,w-a} (T_{a2} - T_w) \\ &+ DA_w \rho_w [L_w + C_{pv} (T_w - T_a)] \frac{dM_w}{dt} \\ &+ \alpha_w F_w I_t A_w \tau_c \end{aligned} \quad (8)$$

##### Mass Balance Equation

The accumulation rate of moisture in the air inside the drying unit = Rate of moisture inflow into the drying unit due to entry of the air from the collector - Rate of moisture outflow from the drying unit + Rate of moisture removed from timber inside the drying unit. The mass balance inside the drying unit gives:

$$\rho_a V \frac{dH}{dt} = \rho_a H_{in} V_{in} - \rho_a H_{out} V_{out} + A_w D \rho_w \frac{dM_w}{dt} \tag{9}$$

**Diffusion of Moisture in the Timber**

Moisture movement inside the timber is by diffusion and it is described by Fick's law (Equation 1). The solution of Fick's law (Equation 2) was used to calculate the moisture content inside the timber boards.

**Equilibrium Moisture Content**

Equilibrium Moisture Content ( $M_e$ ) was calculated using the following empirical equation proposed by Simpson [20]:

$$M_e = \left( \frac{K_1 K_2 rh}{1 + K_1 K_2 rh} + \frac{K_2 rh}{1 - K_2 rh} \right) \frac{1800}{W} \tag{10}$$

where

$$K_1 = 4.737027 + 0.0477346 \cdot T_{air} - 0.0005012 \cdot T_{air}^2 \tag{11}$$

$$K_2 = 0.706 + 0.001698 \cdot T_{air} - 0.000005556 \cdot T_{air}^2 \tag{12}$$

$$W = 211.7 + 0.62365 \cdot T_{air} - 0.01853 \cdot T_{air}^2 \tag{13}$$

$T_{air}$  is drying air temperature (°C) and rh is relative humidity (decimal).

**Model Parameters**

The radiative heat transfer coefficient between the roof and the absorber ( $h_{r,ab-r}$ ) is calculated by using a formula reported in Duffie and Beckman [21] as:

$$h_{r,ab-r} = \frac{\sigma \cdot (T_r^2 + T_{ab}^2)(T_r + T_{ab})}{\frac{1}{\epsilon_r} + \frac{1}{\epsilon_{ab}} - 1} \tag{14}$$

$\sigma$  is the Stefan-Boltzmann constant ( $5.67 \times 10^{-8} \text{ W} \cdot \text{m}^{-2} \cdot \text{K}^{-4}$ ),  $\epsilon_r$  and  $\epsilon_{ab}$  are the emissivities of the roof and the absorber, respectively.  $T_r$  and  $T_{ab}$  are the temperatures of the roof and the absorber in K, respectively.

The radiative heat transfer coefficient between the roof and the sky [21] ( $h_{r,r-s}$ ) is given by

$$h_{r,r-s} = \sigma \epsilon_r (T_r^2 + T_s^2)(T_r + T_s) \tag{15}$$

The sky temperature ( $T_s$ ) is computed from

$$T_s = 0.0552 \cdot T_{am}^{1.5} \tag{16}$$

where  $T_{am}$  is ambient air temperature (K).

The convective heat transfer coefficients between the timber and the air inside the drying unit is calculated from the following relationship:

$$h_{c,w-a} = \frac{Nu k_a}{D_h} \tag{17}$$

where Nu is the Nusselt number,  $k_a$  is the thermal conductivity of the air.  $D_h$  is the hydraulic diameter for calculating the convection heat transfer between the timber boards and air inside the drying unit.

The Nusselt number is calculated from a formula reported by Sartori [22] as:

$$Nu = 0.0369 \cdot Re^{0.8} \cdot Pr^{\frac{1}{3}} \tag{18}$$

where Re is the Reynolds number and  $Pr$  is Prandtl number:

**Solution Procedure**

The system of heat balance equation for the collector (Equations 3 to 5) was solved numerically using the finite difference technique. The collector was divided in N sections along the length of the collector. The differential Equations 3 to 5 were transformed into a system of finite difference equation for all N sections. These were solved simultaneously by the Gauss-Jordan elimination method. The solution of the system of the equations gave the value of the outlet air temperature of the collector and it was used as input data for the system of equation for the drying unit.

For the drying unit, it was assumed that the spatial variation of all drying parameters along the length of the drying unit is negligible and there is only temporal variation of these parameters. The solution procedure started with the numerical calculation of moisture distribution in the timber using Equation 2 and the diffusivity obtained from the experiments in Section 2. The values of the moisture content in the timber were averaged to obtain the moisture content of the timber boards ( $M_w$ ). Then, the change in moisture content of the timber boards  $\Delta M_w$  for a time interval  $\Delta t$  were calculated. Afterwards, the system of equation consisting of Equations 6 to 8 were expressed in the matrix form for the time interval  $\Delta t$  as:

$$\begin{bmatrix} a_{11} & a_{12} & a_{13} \\ a_{21} & a_{22} & a_{23} \\ a_{31} & a_{32} & a_{33} \end{bmatrix} \begin{bmatrix} T_{a2} \\ T_w \\ T_f \end{bmatrix} = \begin{bmatrix} b_1 \\ b_2 \\ b_3 \end{bmatrix} \tag{19}$$

This system of equation were solved by the Gauss-Jordan elimination method using the recorded values for drying air temperature, relative humidity and the change in moisture content of the timber ( $\Delta M_w$ ) for the given time interval. The equation for the moisture ratio H (Equation 9) was also solved numerically using the value of the moisture change  $\Delta M_w$ . The process was repeated until the final time or moisture content was reached. Computer programs in FORTRAN were developed for this calculation.

## 5. RESULTS AND DISCUSSION

### Diffusivities of Timber

Figure 4 shows the variation of the moisture diffusivity of timber as a function of the reciprocal of absolute drying air temperature.

The diffusivity of the timber is highly dependent on temperature. The diffusivity of timber increased with temperature and it was expressed as a function of temperature using Arrhenius type equation as:

$$D = 7.6 \times 10^{-10} \exp(-476.29/T_{ab}) \quad (20)$$

### Experimental Results

The variations of the solar radiation during solar drying of timber in the drying system is shown in Figure 5. Solar radiation increased sharply from 8 am to 11 am and then gradually reached the peak at noon and dropped sharply at 2 pm. The over-all shape of the variation of solar radiation is sinusoidal. However, there

were some fluctuations for few hours due to clouds. The overall patterns of the cyclic variations of the solar radiation are similar.

Figure 6 shows the variations of temperatures inside the drying unit. The temperature at the inlet of the drying unit increased from 8 am till noon and then decreased in the afternoon. The average rise of temperature at the inlet of the drying section was 8.3 °C (standard deviation, 2.8 °C). The variations of the temperature rise above the ambient temperature with solar radiation is shown in Figure 7 and it shows that temperature rise increases with the solar radiation. The average rise of the temperatures at the outlet of the dryer above the ambient temperature is 5.0 °C (standard deviation, 2.1 °C).

Figure 8 shows the variations of the relative humidity at the inlet and outlet of the drying unit. The relative humidity at the inlet and outlet decreased from 8 AM till the evening for most days of the experiment.

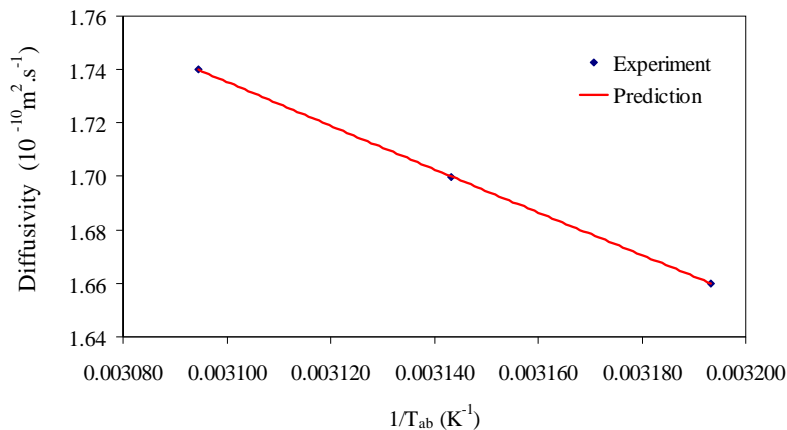


Fig. 4. Variation of the moisture diffusivity of timber as a function of the reciprocal of absolute drying air temperature ( $T_{ab}$ ).

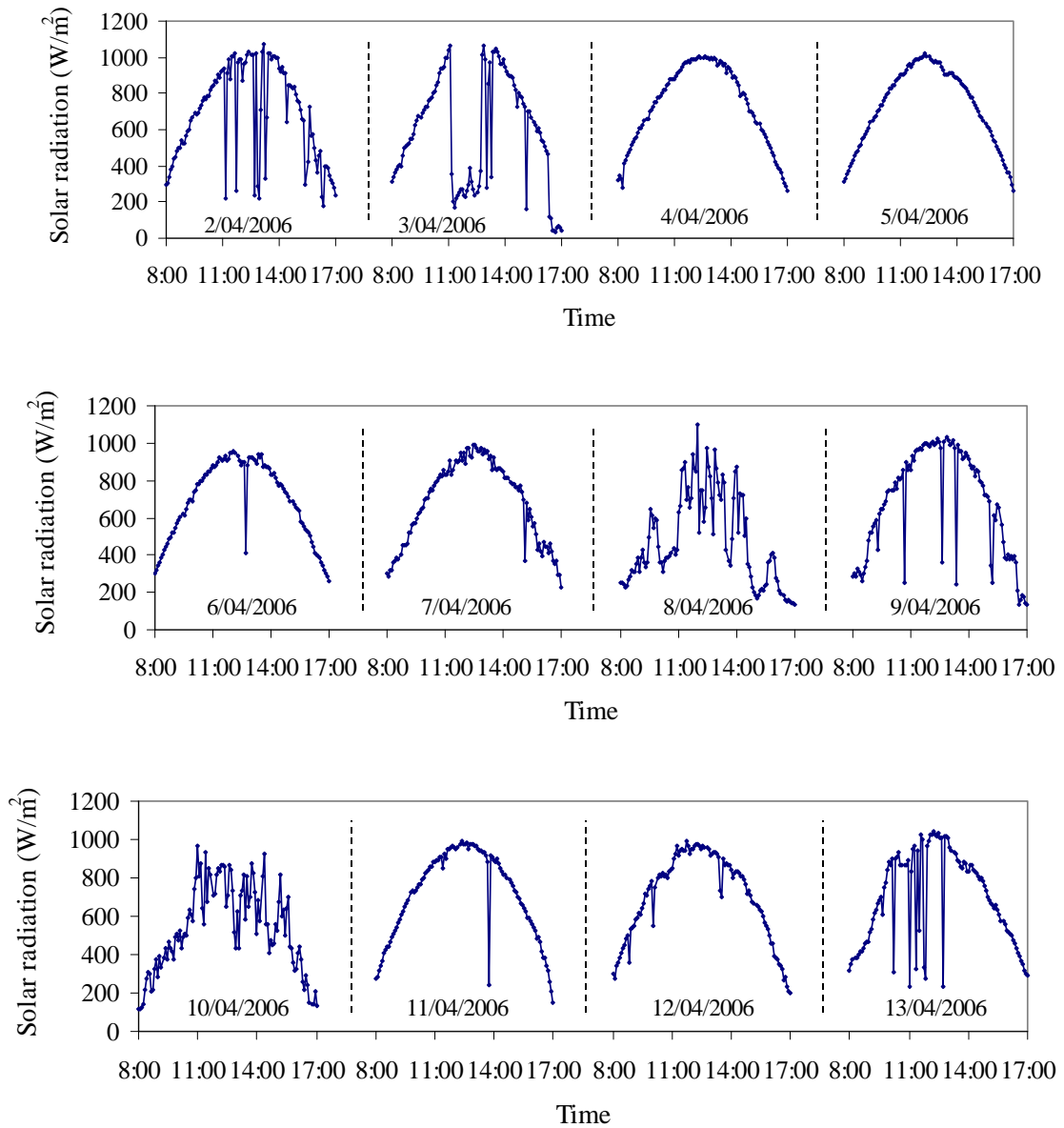
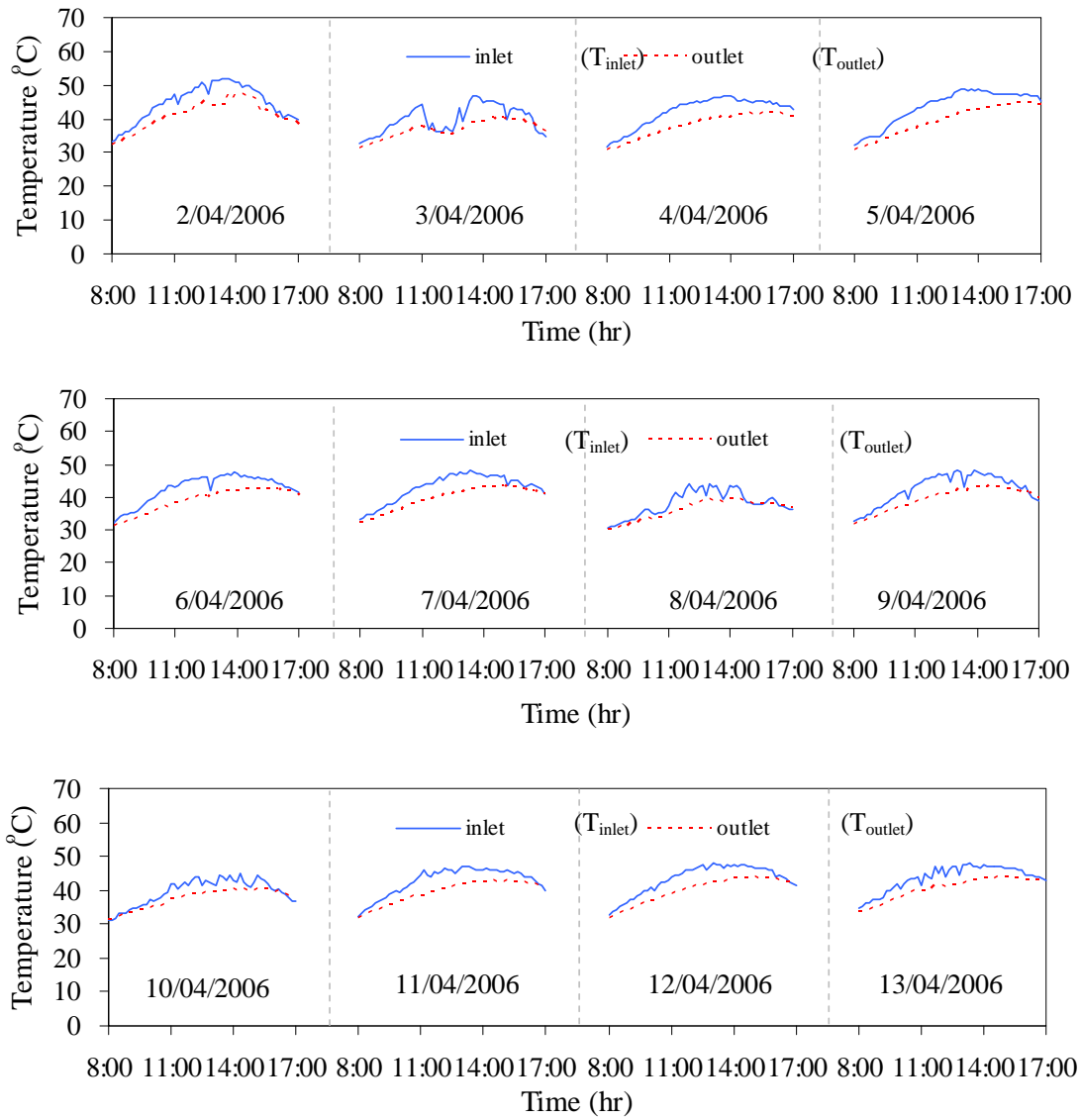
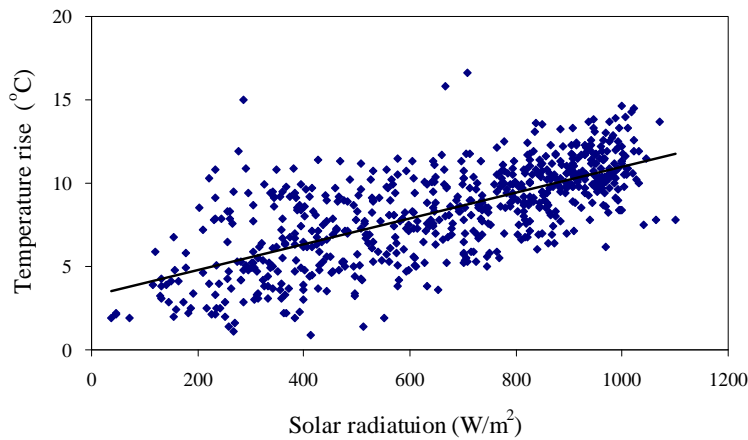


Fig. 5. Solar radiation between 2-13 April 2006.

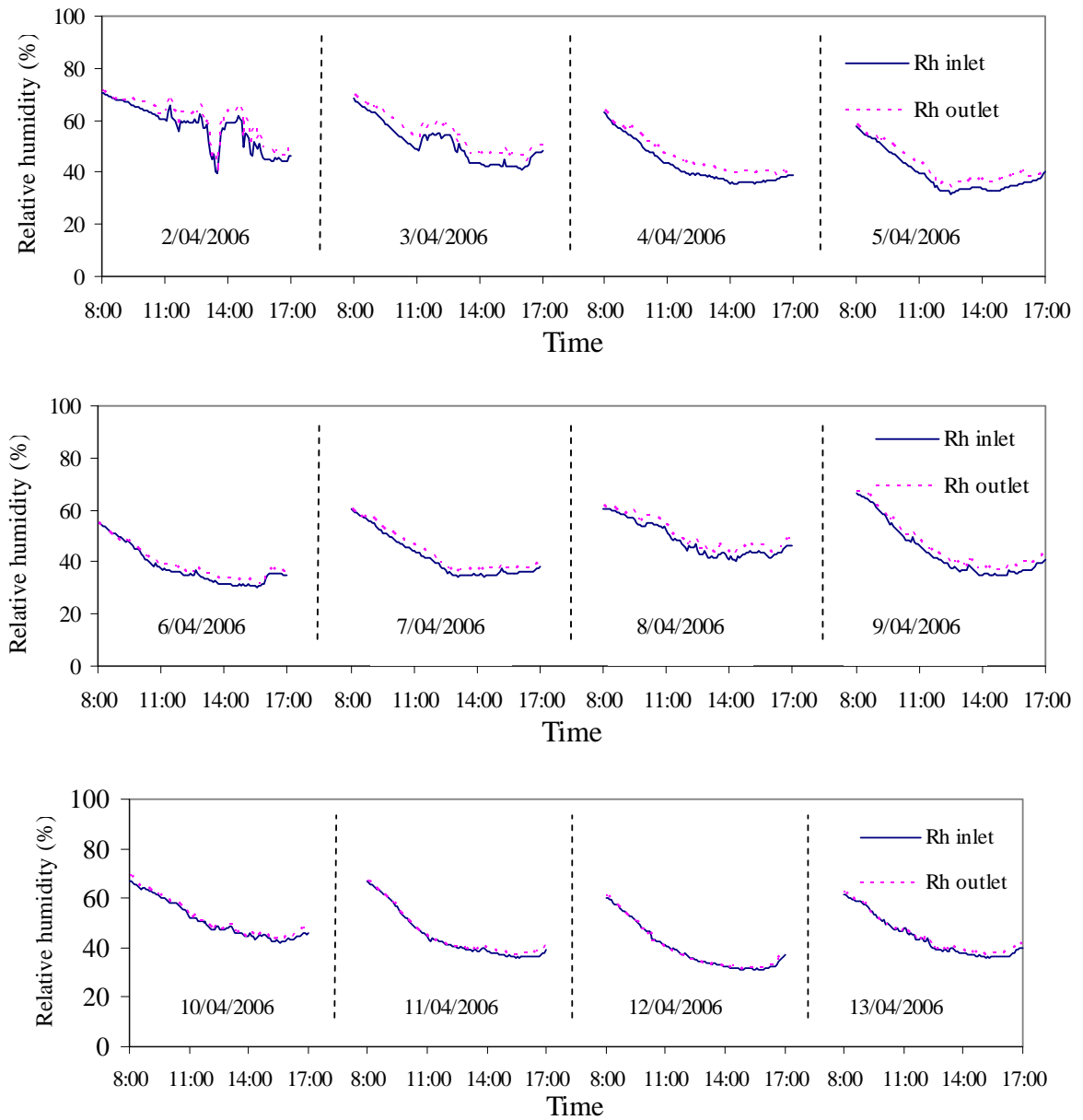


**Fig. 6.** Variations of air inlet temperature ( $T_{in}$ ) and air outlet temperature ( $T_{out}$ ) of the drying unit. (Positions of the measurement is shown in Figure 3).

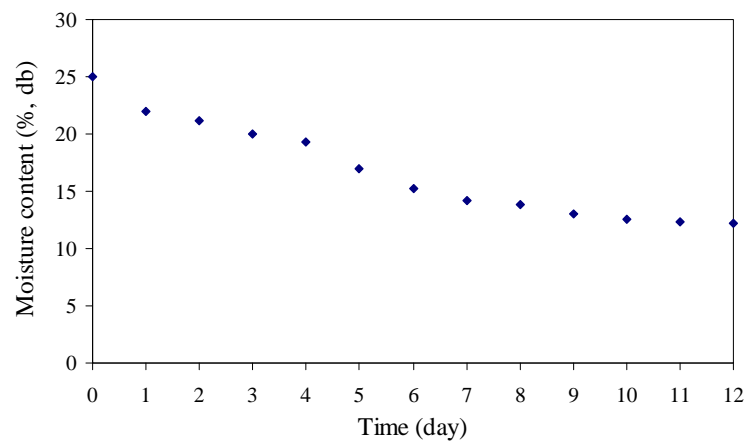


**Fig. 7.** Variations of the temperature rise above the ambient temperature with solar radiation.





**Fig. 8. Relative humidity at the inlet (Rh inlet) and outlet (Rh outlet) of the drying unit.**



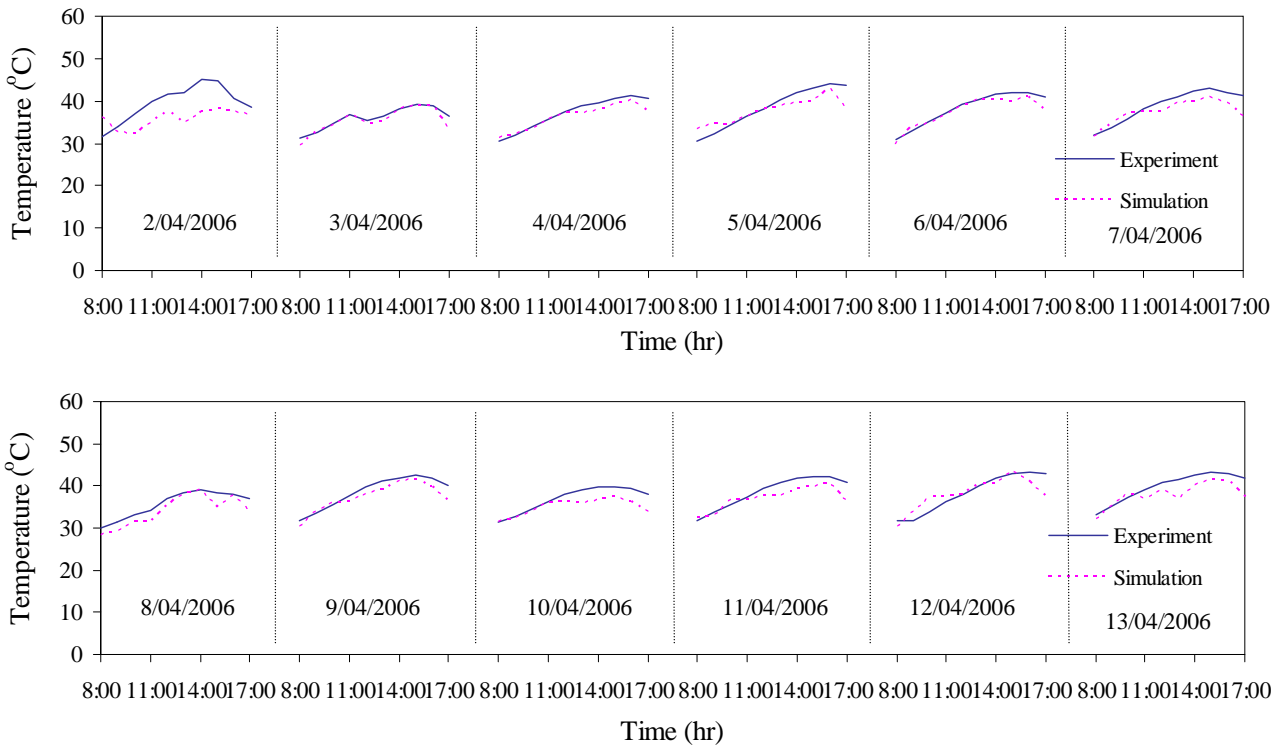
**Fig. 9. Variation of the moisture content of the timber.**

Figure 9 shows the variations of the moisture content of the timber at the middle of the dryer. The moisture content of the timber decreased from 25% (db) to 12.2% (db) in 12 days.

**Simulation Results**

The model was simulated with data for the experimental conditions and the model predictions were compared with experimental data. Figure 10 shows a comparison between the predicted and experimental temperature values for solar drying of timber for twelve consecutive days. The agreement between the predicted and observed values is good and the predicted temperatures show similar cyclical patterns to those of measured temperatures. The root mean square difference of the prediction of the model is 5.7%. Figure 11 shows the comparison between the simulated and experimental

moisture contents. The predicted and experimental results are in reasonable agreement. The root mean square error of the prediction of the model is 8.3%. The errors are within the acceptable limits [23]. Thus, this model predicted well the drying behaviour of timber. The model was used to predict moisture content profiles inside the timber board during drying and the simulated moisture profiles are shown in Figure 12. The moisture gradients are more prominent in the early stage of drying which might cause stress and shrinkage. Younsi *et al.* [15] also reported similar patterns of moisture profiles in timber during drying.



**Fig. 10. Comparison between the simulated and experimental temperatures ( $T_{in}$ ).**

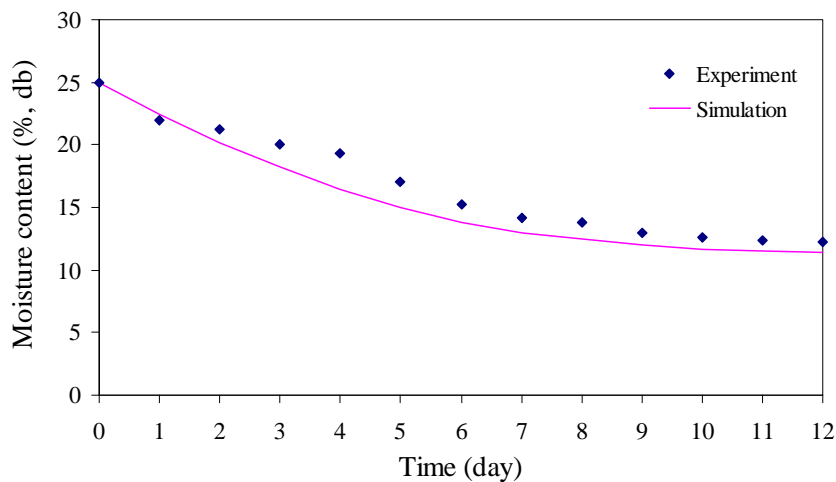


**Fig. 11. Comparison between the simulated and experimental moisture contents.**

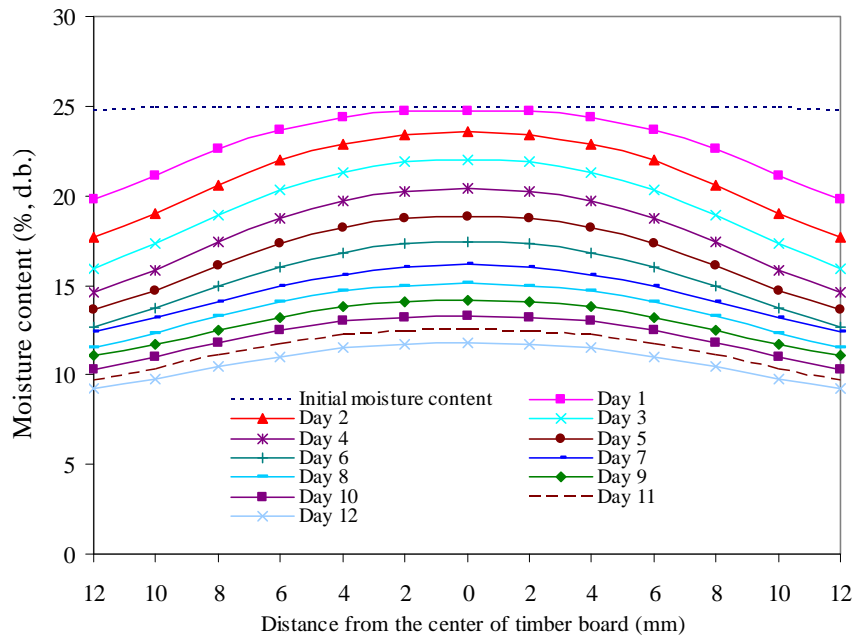


Fig. 12. Moisture content profiles inside the timber during a 12-day drying period.

Table 1 Data on fixed and variable costs and relevant economic parameters.

Items	Costs
- polycarbonate sheets	2,000 USD
- fans	857 USD
- Materials of constructions	11,429 USD
- labour costs	1,143 USD
- Repair and maintenance cost	1% of the capital cost per year
- Expected life span of the dryer	15 years
- Interest rate	7 %
- Inflation rate	3.5%
- Operating cost	1,130 USD per year
- Price of timber to be dried	690 USD / m <sup>3</sup>
- Price of dried timber	770 USD / m <sup>3</sup>

**Economic Evaluation**

For the economic analysis of greenhouse type solar timber dryer, it is assumed that the dryer can be used to dry 380 m<sup>3</sup> of timber round year. Data on fixed and variable costs and relevant economic parameters for estimation of the payback period are given in Table 1.

The payback period of the greenhouse solar timber drying system was estimated to be about 3.6 years. The major items of costs are materials for construction of the structure of the dryer, polycarbonates sheets, fans, operating cost and also labour costs. High capital costs for the construction of the solar timber drying system are the main reason for long payback period. But its profit of timber solar dryer was high. Since drying of timber is an energy intensive operation, drying of timber using

conventional dryer would be much more expensive and such a system is not environmental friendly.

**6. CONCLUSIONS**

The actual performance of the solar drying system shows that the average increase of the drying air temperature is 8.3 °C and the drying time is 12 days in order to reduce the moisture content of the timber to 12.2% (db) from an initial moisture content of 25% (db). The diffusivity of the timber is highly dependent on temperature and it can be expressed as a function of temperature using the Arrhenius type equation. The agreement between the predicted and measured temperatures is good and both the predicted and measured temperatures show similar cyclical patterns. Also the predicted and measured moisture contents are

in reasonable agreement. The payback period is about 3.6 years. The actual performance demonstrates that solar drying of timber is an alternative to either sun or conventional air heated drying and the model can be used to predict the performance of the solar timber drying system.

### NOMENCLATURE

$A_{ab}$	area of the absorber ( $m^2$ )	$k_a$	thermal conductivity of the air ( $W.m^{-2}.K^{-1}$ )
$A_c$	area of the base of the drying unit ( $m^2$ )	$L_w$	latent heat of vaporization of moisture from the timber ( $J.kg^{-1}$ )
$A_f$	area of the concrete floor ( $m^2$ )	$M$	moisture content of the timber (db, decimal)
$A_w$	area of the timber ( $m^2$ )	$M_o$	initial moisture content of the timber (db, decimal)
$A_r$	area of the roof ( $m^2$ )	$M_e$	equilibrium moisture content of the timber (db, decimal)
$C_{pa}$	specific heat of the air ( $J.kg^{-1} K^{-1}$ )	$M_w$	average moisture content of timber board (db, decimal)
$C_{pab}$	specific heat of absorber material ( $J.kg^{-1} K^{-1}$ )	$m_a$	mass of air inside the dryer (kg)
$C_{pff}$	specific heat of the floor ( $J.kg^{-1} K^{-1}$ )	$m_{ab}$	mass of absorber (kg)
$C_{pww}$	specific heat of the timber ( $J.kg^{-1} K^{-1}$ )	$m_r$	mass of the roof (kg)
$C_{ppl}$	specific heat of liquid water ( $J.kg^{-1} K^{-1}$ )	$m_f$	mass of concrete floor (kg)
$C_{prr}$	specific heat of roof material ( $J.kg^{-1} K^{-1}$ )	$m_w$	mass of timber (kg)
$C_{pvv}$	specific heat of water vapour ( $J.kg^{-1} K^{-1}$ )	$Nu$	Nusselt number (-)
$D$	height of the air channel in the drying unit where convective heat transfer between air and the timber takes place (m).	$Pr$	Prandtl number (-)
$D_c$	average distance between the roof and absorber (m)	$Re$	Reynolds number (-)
$D_h$	hydraulic diameter used for the calculation of convective heat transfer between the timber and the air (m)	$rh$	relative humidity (-)
$D_w$	diffusivity of the timber ( $m^2.s^{-1}$ )	$t$	time (s)
$D_p$	thickness of the timber (m)	$T_{am}$	ambient air temperature (K)
$F_f$	fraction of solar radiation falling on the floor (decimal)	$T_{a1}$	temperature air in the collector (K)
$F_w$	fraction of solar radiation falling on the timber (-)	$T_{a2}$	temperature air in the drying unit (K)
$G$	specific flow rate of the air in the collector [ $kg.s^{-1} m^{-2}$ ]	$T_{ab}$	temperature absorber (K)
$H$	humidity ratio of air inside the drying unit ( $kg.kg^{-1}$ )	$T_f$	temperature floor (K)
$H_{in}$	humidity ratio of air entering the drying unit ( $kg.kg^{-1}$ )	$T_g$	temperature of the ground (K)
$H_{out}$	humidity ratio of the air leaving the drying unit ( $kg.kg^{-1}$ )	$T_r$	temperature of the roof (K)
$h_{c,ab-a}$	convective heat transfer between the absorber and the air ( $W.m^{-2}K^{-1}$ )	$T_s$	sky temperature (K)
$h_{c,f-a}$	convective heat transfer between the floor and the air ( $W.m^{-2}K^{-1}$ )	$T_w$	temperature of the timber (K)
$h_{c,w-a}$	convective heat transfer between the timber and the air ( $W.m^{-2}K^{-1}$ )	$U_c$	overall heat loss coefficient from the air inside the drying unit to ambient air ( $W.m^{-2}K^{-1}$ )
$h_{c,r-a}$	convective heat transfer between the roof and the air ( $W.m^{-2}K^{-1}$ )	$V$	volume of the drying unit ( $m^3$ )
$h_{c,r-am}$	convective heat transfer between the roof and the ambient air ( $W.m^{-2}K^{-1}$ )	$V_{in}$	inlet air flow rate ( $m^3.s^{-1}$ )
$h_{D,f-g}$	conductive heat transfer between the floor and the underground ( $W.m^{-2}K^{-1}$ )	$V_{out}$	outlet air flow rate ( $m^3.s^{-1}$ )
$h_{r,ab-r}$	radiative heat transfer between the roof and absorber ( $W.m^{-2}K^{-1}$ )	$W$	width of the air channel in the drying unit where the convective heat transfer between the air and the timber takes place (m)
$h_{r,r-s}$	radiative heat transfer between the roof and the sky ( $W.m^{-2}K^{-1}$ )	$\alpha_{ab}$	absorptance of the absorber (decimal)
$h_{c,r-am}$	convective heat transfer between the roof and the ambient air ( $W.m^{-2}K^{-1}$ )	$\alpha_f$	absorptance of the floor (decimal)
$I_t$	incident solar radiation ( $W.m^{-2}$ )	$\alpha_r$	absorptance of the roof material (decimal)
		$\alpha_w$	absorptance of the timber (decimal)
		$\sigma$	Stefan -Boltzmann's constant ( $W.m^{-2}.K^{-4}$ )
		$\rho_a$	density of air ( $kg.m^{-3}$ )
		$\rho_w$	density of the timber ( $kg.m^{-3}$ )
		$\tau_r$	transmittance of the roof and wall material (polycarbonate) (decimal)
		$\varepsilon_r$	emissivity of the roof (-)
		$\varepsilon_{ab}$	emissivity of the absorber (-)

### ACKNOWLEDGEMENTS

The authors would like to thank the Department of Alternative Energy Development and Efficiency for inviting Silpakorn University to carry out this project. The author would also like to thank Prof. Joachim Müller from Hohenheim University and Dr. Markus Bux from Thermosystem Company for a technical support to this work. We are grateful to Prof. B.K. Bala for valuable advice. Mr. Martin Goedecke and Mr. Niroot Lamlert are acknowledged for their work as research assistants.

## REFERENCES

- [1] Bentayeb, F., Bekkioui, N., Zeghmati, B., 2007. Modelling and simulation of a wood solar dryer in a Moroccan climate. *Renewable Energy* 33(3): 501-506.
- [2] Janjai, S., Laksanaboonsong, J., Nunez, M., Thongsathitya, A., 2005. Development of a method generating operational solar radiation maps from satellite data for a tropical environment. *Solar Energy* 78: 739-751.
- [3] Bala, B.K., 1998. *Solar Drying Systems*. Udaipur, India: Agrotech Publishing Academy.
- [4] Sattar, M.A., 1989. Construction and operation of solar kiln for seasoning timber in Bangladesh. *RERIC International Energy Journal* 7(2): 42-49.
- [5] Haque, M.N., and T.A.G. Langrish, 2003. Mathematical modelling of solar kilns for drying timber: simulation and experimental validation. *Drying Technology* 21(3): 457-477.
- [6] Hewla, N.H., Khater, H.A., Enayet, M.M., and Hashish, M.I., 2004. Experimental evaluation of solar kiln for drying wood. *Drying Technology* 22(4): 703-717.
- [7] Khater, H.A., Helwa N.H., Enayet M.M. and Hashish M.I., 2004. Optimization of a solar kiln for wood drying. *Drying Technology* 22(4): 677-701.
- [8] Awadalla, H.S.F., El-Dib, A.F., Mohamad, M.A., Reuss, M., Hussein, H.M.S., 2004. Mathematical modelling and experimental verification of wood drying process. *Energy Conversion and Management* 45: 197-207.
- [9] Haque, M.N., and T.A.G. Langrish, 2005. Assessment of the actual performance of an industrial solar kiln for drying timber. *Drying Technology* 23(7): 1541-1553.
- [10] Pang, S., 2007. Mathematical modeling of kiln drying of softwood timber: model development, validation, and practical application. *Drying Technology* 25: 421-431.
- [11] Taylor, K.J., and A.D. Weir, 1985. Simulation of a solar timber drier. *Solar Energy* 34(3): 249-255.
- [12] Keey, R.B., and S. Pang, 1994. The high-temperature drying of softwood boards: A kiln-wide model. *Chemical Engineering Research and Design* 72(A6): 741-753.
- [13] Pang, S., and A.N. Haslett, 1995. The application of mathematical models to the commercial high-temperature drying of softwood lumber. *Drying Technology* 13(8-9): 1635-1674.
- [14] Younsi, R., Kocaefe, D., and Kocaefe, Y., 2006. Three-dimensional simulation of heat and moisture transfer in wood. *Applied Thermal Engineering* 26(11-12): 1274-1285.
- [15] Younsi, R., Kocaefe, D., Poncsak, S., and Kocaefe, Y., 2007. Computational modeling of heat and mass transfer during the high temperature heat treatment of wood. *Applied Thermal Engineering* 27: 1424-1431.
- [16] Minea, V., 2008. Energetic and ecological aspects of softwood drying with high-temperature heat pumps. *Drying Technology* 26(11): 1373-1381.
- [17] Ceylan, I., Aktas, M., and Dogan, H., 2007. Energy and exergy analysis of timber assisted heat pump. *Applied Thermal Engineering* 27: 216-222.
- [18] Luna, D., Nadeau, J.P., and Jannot, Y., 2008. Solar timber kilns: state of the art and foreseeable developments. *Renewable and Sustainable Energy Reviews* 13: 1446-1455.
- [19] Guarte, R.C., Muhlbauer, W., and Kellert, M., 1996. Drying characteristics of copra quality of copra and coconut oil. *Postharvest Biology and Technology* 9: 361-372.
- [20] Simpson, W.T., 1971. Equilibrium moisture content prediction for wood. *Forest Products Journal* 21(5): 48-49.
- [21] Duffie, J.A., and W.A. Beckman, 1991. *Solar Engineering of Thermal Processes*. Wiley & Sons, New York.
- [22] Sartori, E., 2006. Convection coefficient equations for forced air flow over flat surfaces. *Solar Energy* 80: 1063-1071.
- [23] O'Callaghan, J.R., Menzies, D.J., and Bailey, P.H., 1971. Digital simulation of agricultural drier performance. *Journal of Agricultural Engineering Research* 16(3): 223-244.

